JOURNAL OF COMPUTATIONAL PHYSICS 92, 82–105 (1991)

On the Adoption of Velocity Variable and Grid System for Fluid Flow Computation in Curvilinear Coordinates

WEI SHYY

Department of Aerospace Engineering, Mechanics, and Engineering Science, Universtity of Florida, Gainesville, Florida 32611

AND

THI C. VU

Dominion Engineering Works, GE Canada, Lachine, Quebec, Canada H8S 2S8

The issues of adopting the velocity components as dependent velocity variables, including the Cartesian and culvilinear ones, for the Navier–Stokes flow computations are investigated. The viewpoint advocated is that a numerical algorithm should preferably honor both the physical conservation law in differential form and the geometric conservation law in discrete form. It is demonstrated that with the curvilinear velocity vectors the curvatures of the grid lines introduce extra source terms into the governing equations. With the Cartesian velocity vector, on the other hand, the governing equations in curvilinear coordinates can retain the full conservation-law form and honor the physical conservation laws. The nonlinear combinations of the metric terms also cause the algorithms based on curvilinear velocity components to be more difficult to satisfy the geometric conservation law and, hence, more sensitive to grid skewness effect. For the combined utilization of the Cartesian velocity vector and the staggered grid arrangement, the implications of spurious pressure oscillation arising from the 90° turning are discussed. It is demonstrated that these spurious oscillations can possibly appear only under a very specific circumstance, namely, the meshes in the region with 90° turning must be parallel to the Cartesian coordinates and of uniform spacing along coordinates; otherwise no spurious oscillations can appear. Several flow solutions for domain with 90° and 360° turnings are presented to demonstrate that satisfactory results can be obtained by using the Cartesian velocity components and the staggered grid arrangement.

1. INTRODUCTION

The computational algorithms utilizing a curvilinear body-fitted coordinate system for Navier–Stokes fluid flow in irregular geometries have been under intensive development recently. Several alternatives have been reported; some of them have been cited by Karki [1], Patankar [2], and Yang *et al.* [3]. One important issue in developing appropriate algorithms is related to the choice of dependent variables for the velocity vector. In gross terms, one has the option of using the

0021-9991/91 $3.00

Cartesian, contravariant, or covariant velocity components as the primary variables. Although comments have been made with regard to the suitability of each of these choices, they are mostly speculations and no studies have convincingly clarified this somewhat confusing issue. For example, both Karki and Yang *et al.*, referred to one particular algorithm developed in [4–6] which uses a staggered grid (Fig. 1) arrangement similar to that for the Cartesian coordinates [7] and stores one Cartesian component at each control- (or finite-) volume face. There were several comments made by them about the algorithm that can be summarized as follows: (i) This type of algorithm is valid only for configurations which do not deviate severely from a Cartesian geometry [1]. (ii) There are other difficulties such as the lack of diagonal dominance in the pressure equation unless the non-orthogonal terms are ignored in the course of the iterative solution [1]. (iii) Difficulties also arise when the grid lines turn 90° from the original orientations, and then the beneficial effects of the grid staggering are lost [1, 3, 8]. Similar observations with regard to 90° turning have also been made by one of the present authors in [6], before the aforementioned references were published.

However, the algorithm developed in [4–6] has not only been successfully applied to a wide variety of 2–D and 3–D flow configurations with substantial complexities, including diffuser [9], cascade of turbine blade [10], gas turbine combustor [11], and natural convection in high pressure discharge lamp [12]. It has also been extended to compute flow with a wide range of Mach numbers ranging from incompressible to hypersonic [13, 14]. Furthermore, after the results presented in [6] have been published flows with 90° turning have also been computed and very favorable theory/data comparisons obtained using very similar algorithms with somewhat different grid arrangements [15, 18]. It appears that the concerns raised in [6] about the spurious pressure made may not be as well founded as one may imagine. Evidently, the choice of primary dependent variables for velocity vector is a complicated issue which deserves some more careful investigation.

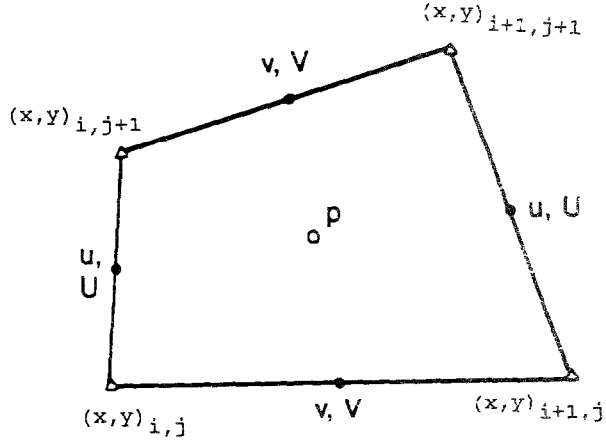

FIG. 1. Configuration of a staggered grid system.

The present study attempts to address the issues of adopting the velocity components in curvilinear grid systems, such as the Cartesian, contravariant, or covariant velocity components. Both basic analyses and relevant examples will be used to illustrate and, hopefully to clarify, the technical difficulties associated with this issue. In the meantime, a related and equally important issue, namely, the utilization of the so-called staggered and non-staggered grid systems [4, 7], will also be addressed.

2. Basic Analysis

Before a detailed discussion is presented, it seems beneficial to give a brief account of the governing equations and numerical algorithm developed in [4–6] designed to solve these equations. The equations to be solved are the steady-state Navier–Stokes equations along with related transport equations of the mass continuity, linear momentum, energy, species concentrations, and so on. Detailed accounts of those equations, including basic derivation procedure, can be found from many sources such as the books by Bird *et al.* [24], Kuo [25], and Rosner [26]. The steady-state governing equations for the mass continuity and momentum transport in two-dimensional Cartesian coordinates are given as an example,

$$\frac{\partial(\rho u)}{\partial x}+\frac{\partial(\rho v)}{\partial y}=0 \tag{1}$$

$$\frac{\partial(\rho u^2)}{\partial x}+\frac{\partial(\rho uv)}{\partial y}=-\frac{\partial p}{\partial x}+\frac{\partial \tau_{xx}}{\partial x}+\frac{\partial \tau_{xy}}{\partial y}+\rho B_x \tag{2}$$

$$\frac{\partial(\rho uv)}{\partial x}+\frac{\partial(\rho v^2)}{\partial y}=-\frac{\partial p}{\partial y}+\frac{\partial \tau_{xy}}{\partial x}+\frac{\partial \tau_{yy}}{\partial y}+\rho B_y, \tag{3}$$

where ρ, u, v, p, τ, B designate, respectively, fluid density, u-velocity component, v-velocity component, static pressure, shear stress, and body force. The subscripts associate with τ and B indicate that they are elements of second-order tensor and vector, respectively. Since in many pratical applications the flow configurations do not conform to the Cartesian geometry, appropriate numerical methods must be devised to solve Eqs. (1) to (3) with curvilinear grid lines.

With regard to the numerical algorithm developed in [4–6], a combined use of the Cartesian and controvariant velocity components has been adopted to facilitate the satisfaction of conservation laws that the algorithm is set out to solve in the first place. In more specific terms, the Cartesian velocity components are used in all of the momentum equations as the primary variables. In other equations, including all the scalar variables such as temperature and concentration, the contravariant components resulting from the Cartesian components are employed to evaluate the mass fluxes across each surface of finite volume. One key feature, reported in [5], is to directly employ the contravariant velocity components to yield the velocity

corrections resulting from the pressure correction equation to exactly, in discrete sense, satisfy the continuity equation. Afterwards, a highly efficient iterative procedure called D'Yakonov method [16] is employed to convert the information from the contravariant to the Cartesian velocity components. This type of hybrid formulation is proven to be highly efficient and does not require much of extra computing effords. More importantly, the very reason of devising this hybrid approach is to retain the Cartesian velocity components as primary variables for velocity vector and to satisfy the conservation laws in an efficient manner.

With regard to the staggered grid system employed here, as shown in Fig. 1, the Cartesian velocity components u and v are defined at the middle of east–west and north–south faces, respectively. That is, in 2-D curvilinear coordinates designated as ξ-lines and η-lines, u-components is defined at the middle of η-lines of the mesh, and v-component is defined at the middle of ξ-lines of the mesh. All the scalar variables such as pressure, p, temperature, T, and density, ρ, are located at the geometric center of the four vertices defining the mesh.

First the relationship between the Cartesian (u, v) and contravariant (U, V) velocity components are defined as follows:

$$U = y_\eta u - x_\eta v \tag{4}$$

$$V = -y_\xi u + x_\xi v. \tag{5}$$

Then the continuity equation in ξ- and η-coordinates can be written in the similar form with the contravariant velocity components to that in x- and y-coordinates with the Cartesian velocity components (Eq. (1)), i.e.,

$$(\rho U)_\xi + (\rho V)_\eta = 0, \tag{6}$$

where the subscripts ξ and η, denote the partial derivatives along the curvilinear coordinate lines. With regard to the covariant velocity components, defined as $\tilde{U}$ and $\tilde{V}$ here, i.e.,

$$\tilde{U} = x_\xi u + y_\xi v \tag{7}$$

$$\tilde{V} = x_\eta u + y_\eta v \tag{8}$$

the continuity equation written in the covariant velocity components are

$$(\rho\alpha_1 \tilde{U} + \rho\beta_1 \tilde{V})_\xi + (\rho\alpha_2 \tilde{U} + \rho\beta_2 \tilde{V})_\eta = 0, \tag{9}$$

where

$$\alpha_1 = \frac{q_{11} q_{22}^2}{J}$$

$$\beta_1 = \alpha_1 (\mathbf{e}_\xi \cdot \mathbf{e}_\eta)$$

$$\alpha_2 = \frac{q_{11}^2 q_{22}}{J}$$

$$\beta_2 = \alpha_2 (\mathbf{e}_\xi \cdot \mathbf{e}_\eta)$$

$$q_{11} = (x_\xi^2 + y_\xi^2)^{1/2}$$

$$q_{22} = (x_\eta^2 + y_\eta^2)^{1/2}$$

$$J = x_\xi y_\eta - x_\eta y_\xi;$$

$\mathbf{e}_\xi$ and $\mathbf{e}_\eta$ are unit vectors along ξ- and η-directions, respectively, i.e.,

$$\mathbf{e}_\xi = \frac{x_\xi \mathbf{e}_x + y_\xi \mathbf{e}_y}{q_{11}} \tag{10a}$$

$$\mathbf{e}_\eta = \frac{x_\eta \mathbf{e}_x + y_\eta \mathbf{e}_y}{q_{22}}. \tag{10b}$$

The relevant issues of formulating the pressure correction equation have been discussed in some details by Karki [1] and will not be repeated here. One of the key features is that the coordinate transformation associated with the use of both the Cartesian and contravariant velocity components may introduce the off-diagonal contributions into the pressure correction equation. For 2D case, the pressure correction equation may be of a nine-point structure instead of a five-point structure, as pointed out by Shyy *et al.* [4]. However, it should be pointed out that it is not clear how much extra effort will be needed to handle this extra complexities. For instance, Shyy *et al.* [4] have found that it is very acceptable to simply keep the five-point contributions and to ignore all other off-diagonal terms in the iterative solution procedure. This approach does not affect the final solution but has caused concern regarding the numerical convergence rate, especially under the influence of skewed meshes. The wide variety of applications documented in [8–16] convincingly demonstrate that this procedure is very robust in a wide spectrum of grid skewness. Moreover, one can also resort to a more complicated equation solver than the conventional line-SOR method by retaining all nine-point structure. The relative merits of these approaches may well be problem dependent and they are relevant only to computational efficiency, not computational accuracy. As to the use of covariant velocity components, the extra source generated in the momentum and other transport equations may require explicit treatments. Hence the overall computational efficiency of the whole system of equations is not easy to estimate. This issue will not be further pursued in the present work. What will be the focal point here is the issues related to the computational accuracy.

I. *Physical and Geometric Conservation Laws*

When considering the various possible choices of velocity variables, one of the primary criteria is that in the framework of finite-volume formulation, a fully

conservative-law form of governing equations is usually more desirable since it can satisfy the physical laws more easily and accurately. This consideration has a particularly important implication on the convection terms of the momentum equations since they are nonlinear and are usually the source of numerical difficulty. One example has been given by Chu [23]. With the Cartesian coordinates, the convection terms in Eq. (2) are of the form of $(\rho uu)_x + (\rho vu)_y$, which is fully conservative. In a curvilinear coordinate system, these terms can be transformed in a straightforward manner with the use of the Cartesian velocity components as the primary dependent variables to the form of $(\rho Uu)_\xi + (\rho Vu)_\eta$ which is also fully conservative. However, when either the contravariant or the covariant velocity components are used as the primary dependent variables, the fully conservative form can no longer be guaranteed since the linear momentum is conserved along a straight line, not a curved line. Thus the differential equations for both the contravariant and the covariant velocity components involve the source terms arising from the curvature of the coordinate lines. Furthermore, in the numerical implementation, the contravariant components ρU and ρV on each boundary of the mesh are defined as the mass flux between the two end points of the boundary [4] and their values can artificially change with the mesh spacings. Hence, for the same flowfield the values of those contravariant and covariant velocity components can be greatly affected by the ways that the grid systems are generated. These aspects can cause difficulties in preserving high degrees of numerical accuracy in satisfying the conservation laws.

To demonstrate this point, consider the purely convective equation

$$(\rho uu)_x + (\rho vu)_y = 0. \tag{11}$$

One of the most basic tests of the numerical accuracy of any computational algorithm can be made by generating a grid system with arbitrary skewness and nonuniformity and then to use this grid system to check the numerical accuracy of it by solving a uniform flow field of, say, $\rho = 1$, $u = 1$, and $v = 1$. With this condition, Eq. (11) is trivially satisfied in a differential sense. Hence it serves as a good case to test whether an algorithm can honor the geometric aspect of the conservation laws in discrete form. Here we call this requirement the geometric conservation law [27] since the governing equations retain the conservation law form but contain only the geometric quantities. The transformed equation of Eq. (11) with the Cartesian velocity components as dependent variables in curvilinear coordinates then becomes

$$(\rho Uu)_\xi + (\rho Vu)_\eta = 0, \tag{12}$$

which with the uniform flowfield is reduced to

$$(y_\eta - x_\eta)_\xi + (-y_\xi + x_\xi)_\eta = 0. \tag{13}$$

Referring to Fig. 1, Eq. (13) is discretized as

$$(y_\eta - x_\eta)_e - (y_\eta - x_\eta)_w + (-y_\xi + x_\xi)_n - (-y_\xi + x_\xi)_s = 0, \tag{14}$$

where e, w, n, and s denote the east-, west-, north, and south-face of the mesh, respectively. If a consistent finite-volume formulation is adopted, as shown in [4], by approximating the derivative of the metrics terms in Eq. (14) with the difference between two end points of the mesh line, then Eq. (14) becomes

$$\begin{aligned}
&[(y_{i+1,j+1} - y_{i+1,j}) - (x_{i+1,j+1} - x_{i+1,j})] \\
&\quad - [(y_{i,j+1} - y_{i,j}) - (x_{i,j+1} - x_{i,j})] \\
&\quad + [-(y_{i+1,j+1} - y_{i,j+1}) + (x_{i+1,j+1} - x_{i,j+1})] \\
&\quad - [-(y_{i+1,j} - y_{i,j}) + (x_{i+1,j} - x_{i,j})] = 0
\end{aligned} \tag{15}$$

which is satisfied *exactly*, regardless of how skew or nonuniform the meshes are. It is also noted that one of the merits of this test problem is that since the flowfield is uniform, the whole focal point is directed toward the satisfaction of geometric requirements; other issues such as the appropriate approximation of the convection effects do not arise here.

Since our primary interest is for Navier–Stokes flow computation, it is useful to point out that the above geometric conservation law is applicable to the pressure gradient terms as well. However, the same requirements cannot be rigorously satisfied by the viscous terms due to the appearance of the nonlinear metric products associated with the coordinate transformation of the second-order derivative terms. The detailed information related to viscous term treatment can be found in [4] and will not be repeated for the interest of saving space. (It is, however, a good opportunity here to point out that in [4] there is a typographical error in Eq. (10b), where the sign in front of C^u should be negative instead of being positive.) Overall, one can summarize the situation by stating that with the use of Cartesian velocity components, the Navier–Stokes equations can be written in the strong conservation law form in the curvilinear coordinate system. In terms of numerically satisfying the geometric conservation law, the first-order derivatives, including the convection and pressure terms, can always achieve it. The degree of satisfaction of the viscous terms, on the other hand, is dependent upon the actual grid distribution.

For the use of curvilinear components, say, the contravariant vector, the equation corresponding to Eq. (11) can be obtained by performing a chain- rule type of coordinate transformation,

$$\begin{aligned}
&[\rho U^2/q_{11}]_\xi + \begin{Bmatrix} 1 \\ 1\ 1 \end{Bmatrix} \rho U^2/q_{11} + \begin{Bmatrix} 1 \\ 1\ 2 \end{Bmatrix} \rho UV/q_{11} \\
&\quad + (q_{11}/q_{22})[\rho UV/q_{11}]_\eta + \begin{Bmatrix} 1 \\ 1\ 2 \end{Bmatrix} \rho UV/q_{22} + \begin{Bmatrix} 1 \\ 2\ 2 \end{Bmatrix} \rho V^2 q_{11}/(q_{22})^2 \\
&\quad - (\rho U/q_{11})\, U_\xi - (\rho U/q_{22})\, V_\eta = 0,
\end{aligned} \tag{16}$$

where q_{11} and q_{22} are defined previously, and the Christoffel symbols of the second kind are defined as

$$\begin{Bmatrix} 1 \\ 1\ 1 \end{Bmatrix} = \frac{y_\eta x_{\xi\xi} - x_\eta y_{\xi\xi}}{J} \tag{17a}$$

$$\begin{Bmatrix} 1 \\ 1\ 2 \end{Bmatrix} = \frac{y_\eta x_{\xi\eta} - x_\eta y_{\xi\eta}}{J} \tag{17b}$$

$$\begin{Bmatrix} 1 \\ 2\ 2 \end{Bmatrix} = \frac{y_\eta x_{\eta\eta} - x_\eta y_{\eta\eta}}{J}. \tag{17c}$$

It is now obvious that Eq. (16) not only possesses more terms than Eq. (11), but more critically it contains source terms resulting from the curvature of the coordinate line. Hence, it is no longer of the fully conservative form which can cause difficulties with the finite-volume formulation, especially if the grid system contains substantial nonuniformity and skewness. The fact that q_{11} and q_{22} are nonlinear with respect to the metrics terms resulting from the coordinate transformation further compounds the difficulty of exactly satisfying the conservation law in a discrete manner. A similar case can be made to the equation cast in terms of covariant velocity components.

It should be emphasized that in the context of using curvilinear velocity components, there are many possible ways to manipulate the governing equations and Eq. (16) is not the only form that has been adopted in numerical computations. For instance, a very interesting way of utilizing the covariant velocity components as the primary dependent variable which avoids complicated tensor manipulation is given by Karki [1]. In [1], the discretized equations for the covariant velocity components are obtained by an algebraic manipulation of the corresponding equations for the Cartesian velocity components which avoids any reference to the differential form of the conservation equation for the curvilinear velocity components. The momentum equations adopted in [1] are derived based on a local coordinate system in which all the velocity appearing in any given discrete equation follows the direction of the velocity vector at the center point of each control volume. By starting this way, the spirit of linear momentum conservation is retained in each equation and thus the source terms from the curvature effects are not involved. Hence the appearance of the conservation law form is formally preserved. However, in order to be able to actually solve the discretized equations, more manipulations are needed (as shown in Eqs. (3)–(74) of [1]), since each linear discretized equation now contains more than one family of velocity components. In the final form, curvature terms reemerge, albeit in a different formulation procedure.

The other observation related to satisfaction of the geometric conservation law can be made by studying the continuity equation written in terms of the covariant velocity components. Equation (9) demonstrates that the conservation law can be preserved in differential form for the covariant velocity components. However, because the terms α and β involve nonlinear combinations of metrics terms, the

geometric conservation law cannot be always honored in a skewed mesh system. It is clear that, since the physical conservation laws are the ones that we ultimately strive to satisfy, the numerical algorithms not only preferably should be written in strong conservation law in differential form, but also should satisfy the geometric conservation law in discrete manners. The latter requirement cannot be satisfied as long as the equations contain nonlinear metric terms, regardless of whether the fully conservation law form is adopted in the differential equations or not.

II. *Orientation Dependency*

Besides the satisfaction of conservation laws, another issue relevant to the choice of velocity variables is the dependency of numerical accuracy of the orientation of grid lines. In this regard, since the Cartesian velocity components are always referred to a fixed orientatin throughout the whole domain and, on the other hand, both the covariant and contravariant velocity components are defined in terms of the local coordinates and hence do not possess any preferred direction, it appears that the employment of the latter as dependent variables is more satisfactory. More importantly, as suggested in [1, 3, 8, 9], with the combined use of the Cartesian velocity components and the staggered grid arrangement, difficulties arise when the grid lines turn 90° from the original orientations, and then the beneficial effects of the grid staggering are lost. These are legitimate and important points that deserve some more investigation.

First, it should be pointed out that while the employment of the Cartesian velocity components yields results that are coordinate orientation dependent, they nevertheless all possess the same order of accuracy in the sense of Taylor series expansion and mesh size. Hence the important requirement that the results can be improved at the same rate as the meshes are refined is met. As to the issue of 90° turning, Fig. 2 is used to illustrate the point. It is seen that the original characteristics of the staggered grid arrangement can be largely lost with a 90° turning where the u-velocity is located where, nominally, v-velocity is located, and vice versa. However, does this mean that the pressure gradients which drive these velocities will be errorously evaluated? The answer is "not necessarily." It is noted that the pressure gradient term along the x-direction is of the form of $\partial p/\partial x$. After the transformation from $x-y$ coordinates to the curvilinear $\xi-\eta$ coordinates, the same pressure gradient term driving the u-velocity now appears as $y_\eta p_\xi - y_\xi p_\eta$. With a complete 90° turning *and* the fact that the ξ-lines are parallel to the y-lines, y_η is zero and the only contribution of the pressure gradient term for u-velocity comes from the $y_\xi p_\eta$ term. Here y_ξ is the projected length of mesh boundary on which the pressure force is exerted. An identical argument can be made for the v-momentum equation whose pressure gradient terms appear in the form of $x_\xi p_\eta - x_\eta p_\xi$.

As indicated in Fig. 2(b), the p_η term with 90° turning can be approximated by a six-point averaging/differencing procedure. That is, for the finite-volume cell of the variable $u_{i+1,j+1}$, p_η can be approximated by the difference of the weighted four-point averaging of ($p_{i+1,j+1}$, $p_{i+1,j}$, $p_{i,j}$, $p_{i,j+1}$,) and the weighted four-point

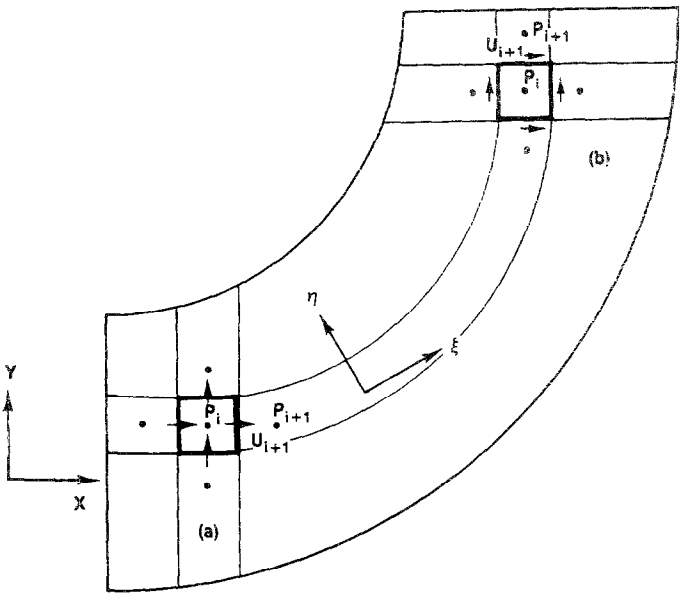

FIG. 2. Effect of control volume orientation on the effectiveness of the grid staggering: (a) effective grid staggering ($\xi = x, \eta = y$); (b) ineffective grid staggering ($\xi = y, \eta = x$).

averaging of ($p_{i+1,j}$, $p_{i,j}$, $p_{i+1,j-1}$, $p_{i,j-1}$,). Hence if the metric term y_ξ is of constant value in the grid system then the resulting approximation of p_η for the variable of $u_{i+1,j+1}$ will be the difference between $(p_{i+1,j+1} + p_{i,j+1})$ and $(p_{i+1,j-1} + p_{i,j-1})$, which means that a "chequerboard" type of spurious pressure oscillations [7, 18] may be acceptable as numerical solutions. For example, with a uniform pressure field, i.e., zero pressure gradient, any alternating values of pressure field that gives zero pressure gradient based on the aforementioned four-point approximation scheme will be satisfactory as far as the momentum equations are concerned.

One would then like to know under what circumstances this spurious mode of pressure oscillation will not appear. It is noted that with the combined use of the staggered grids and the aforementioned interpolation scheme for pressure gradients, even with constant y_ξ, the chequerboard pressure oscillations cannot appear as long as y_η is not identical to zero in the region of 90° turning. Similar observation can be made for the v-momentum equation. That is, if either x_ξ is not identical to zero or x_η is not a constant in the region of 90° turning, the staggered grid arrangement can prevent the chequerboard oscillations from appearing. With these points in mind, we conclude that the chequerboard pressure oscillations can appear possibly only when the meshes in the region of 90° turning are both of the Cartesian geometry and of uniform spacing along all coordinates. This conclusion can be supported by considering the three possibilities that y_ξ is a constant: (i) Cartesian grids, (ii) non-Cartesian but η-lines are parallel to x-lines, and

(iii) non-Cartesian but η-lines are parallel to each other. These three possibilities are illustrated in Fig. 3.

In (i), both y_η and x_ξ are zero. However, unless the meshes are of uniform spacings along both ξ- and η-directions, y_ξ and x_η are not both of constant values, hence a weighted interpolation scheme for pressure gradients effetively rules out the possibility of chequerboard pressure oscillations. In both (ii) and (iii), where the meshes are not Cartesian, the 90° turning of the solid boundaries assures that the chequerboard oscillations cannot appear since in both cases it is impossible for y_η

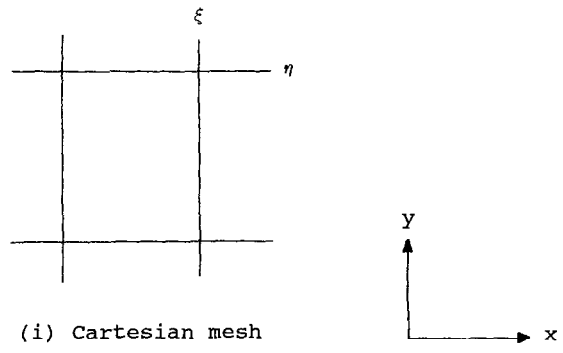

FIG. 3. Three circumstances under which y_ξ is a constant.

and x_ξ to be identical to zero as well as for y_ξ and x_η to be constant values. In summary, the problem of 90° turning associated with the use of the Cartesian velocity components and the staggered grid arrangement appears far less severe. It is shown that the spurious pressure oscillations can possibly appear only under the specific condition that the meshes are parallel to the Cartesian coordinates and uniform along all coordinate lines. This is a rather stringent restriction, since the non-uniform meshes are almost invariably found in complex flow computations to resolve the varying length scales and flow structures. Hence the staggered grid arrangement is still of great value in the present algorithm, especially for boundary treatments.

It is useful at this point to draw some more comparisons between the staggered and nonstaggered grid systems. First, as long as the metric terms x_ξ, x_η, y_ξ, and y_η are all non-constants, both the staggered and nonstaggered grid systems are free

terms are constant, then an alternative discretization procedure is needed to appropriately handle the pressure terms in the nonstaggered grid system. In staggered grid system, on the other hand, the potential problems of producing the spurious pressure oscillations are fundamentally caused by the displaced grid arrangment. An easy cure can be made by simply turning the flow geometry relative to the Cartesian coordinates so that the above undesirable phenomenon does not occur in the first place. Referring to Fig. 2, as long as ξ-lines in the inlet region are not parallel to x-lines, the spurious pressure oscillations will not occur. It is emphasized that since the orientation of the flow geometry can be defined arbitrarily with respect to any coordinate system, there is no reason to always insist on defining the ξ-lines in the inlet region to be parallel to x-lines. For the example shown in Fig. 2, one can simply define the x-coordinate to be, say, of 45° instead of parallel, to the inlet of the channel; the difficulty of velocity decoupling will then disappear regardless of the grid distributions.

In summary, in any orientation, if the metric terms between (x, y) and (ξ, η) coordinates are nonconstant, then the spurious pressure oscillations do not appear in both the staggered and nonstaggered grid. For the staggered grids, moreover, the problem of spurious pressure oscillation can be prevented even with the constant metrics terms. One can simply define the curvilinear coordinates to be non-parallel to the Cartesian coordinates.

Besides the algorithms utilizing the staggered grid arrangement, a few methods based on the nonstaggered grid arrangement have also been proposed [19, 20]. These methods require special procedures to prevent the decoupling of the velocity and pressure fields from exhibiting the chequerboard oscillations. For example, in [19] an explicit fourth-order pressure dissipation term is added to the pressure correction equation to suppress the spurious oscillations. However, with the use of finite mesh sizes, in reality the artificially added fourth-order gradient term may not be smaller than the original second-order gradient term, especially when there are large pressure gradients present in the flowfield, as demonstrated by a Fourier type

of analysis [21]. Hence the actual degrees of numerical accuracy may be affected by the numerical smoothing procedure. Furthermore, it is also well known [22] that artificially generated boundary conditions are needed for the pressure in a non-staggered grid system. With the use of the staggered grid system, there is no need to devise artificial boundary conditions for the pressure correction equation [4] regardless the orientation of the coordinate system. In terms of the momentum equations, since in general both P_ξ and P_η terms appear in both u- and v-momentum equations, some extrapolation procedures will still be needed.

3. *Pratical Flow Examples*

To demonstrate the pratical implications of the present algorithm, several examples of direct relevance with the aforementioned issues will be presented. Results of flows in domains with 90° and 360° turnings are shown here. These flow configurations are found in the hydraulic turbine system, as schematically shown in Fig. 4. For the flow through the casing, which directs the water circumferentially into the turbine and runner, a 360° turning of the domain is encountered. Downstream of the runner, a draft tube typically of 90° turning is used to recover the static pressure from the kinetic energy. Both the casing and the draft tube pose direct tests of the issues related to the 90° degree turning of the present algorithm. All the results shown in the following have been obtained by using the Cartesian velocity components and the staggered grid system. No artificial smoothing or interpolation procedures were needed to yield the solutions.

A. 3*D Casing*

The schematic representations of the casing, including the overall geometry, the evolution of the size of cross section, and representative grid distributions are summarized in Fig. 5. The water enters from the upstream inlet and exists through the inner circumferencial surface. The grid system is of the size of $95 \times 21 \times 13$ nodes.

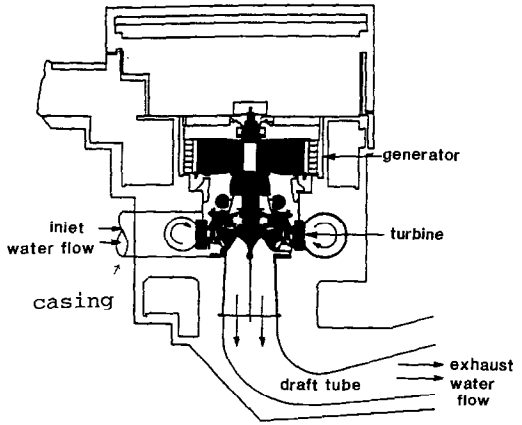

FIG. 4. Schematic of hydraulic turbine system.

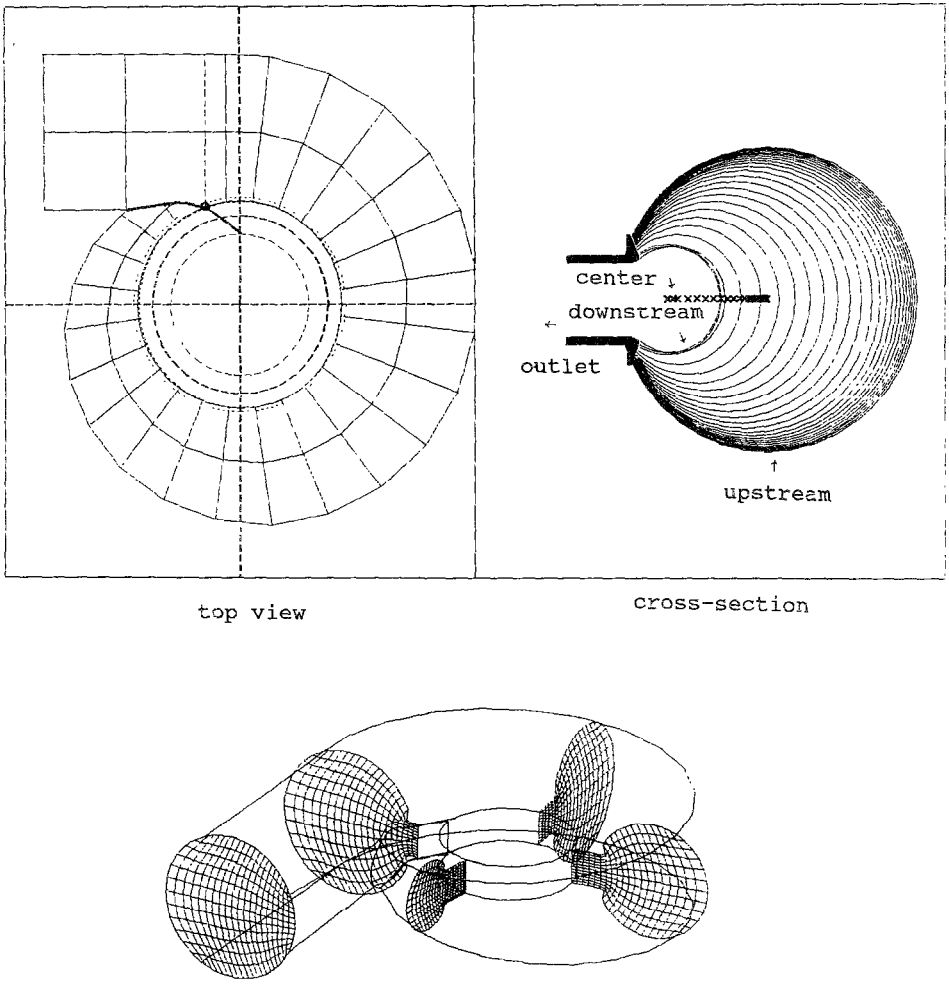

FIG. 5. Geometry and grid system of casing.

Figure 6 shows a top-view of a casing with smooth and continuous turning. Figure 7 shows the computed particle trajectories in short time durations and static pressure distributions in the middle top-view plane for a laminar flow. For the present problem, a key dimenionless parameter characterizing the flow behaviour is the Reynolds number, Re, defined as

$$\mathrm{Re} = uL/\nu$$

where u, L, and ν are the characteristic values of velocity, length, and kinematic

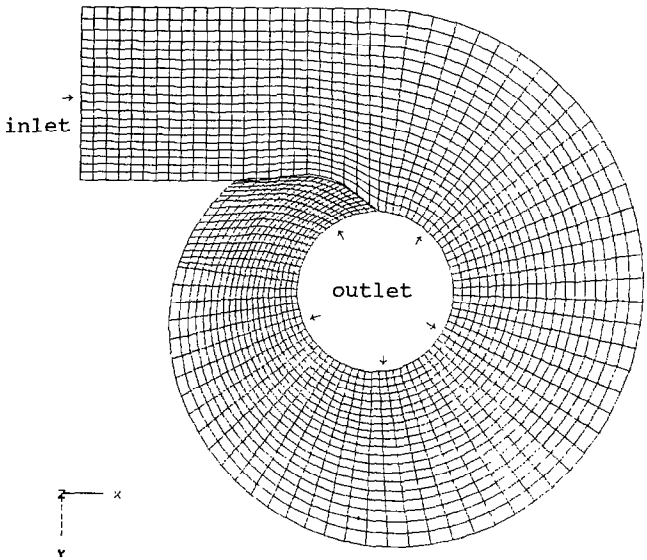

FIG. 6. Grid system in top-view plane of a casing with smoothly varying wall contours.

viscosity of the flow, respectively. The Reynolds number based on the fluid kinematic viscosity, the incoming uniform velocity and the inlet diameter of the present case is 100. It can be seen that, throughout the whole flow domain, no spurious oscillations are present in the numerical solution. With the given Reynolds number, the flow in the casing shows combined characteristics of that through a pipe (in the outer portion of the casing) and that into a sink (in the inner portion of the casing).

Is is worth pointing out that, in general, the conventional averaging process may not be a good practice because there are circumstances that the actual flow device may produce physical oscillations. The casing is such an example. Due to the structure and manufacturing consideration for its large size, it is common to divide the circular boundary into a series of interconnecting straight segments. Figure 8 shows a casing with geometry similar to that in Fig. 6, but the whole 360° of continuous and smooth turning is now replaced by 20 straight segments, each one spanned over 18°. The computed particle trajectories and static pressure distributions for the same inlet condition and Reynolds number in the present geometry are shown in Fig. 9. The slope discontinuity between the two consecutive segments causes the pressure distribution to have less uniform gradient in the outer domain compared to Fig. 7. Calculations have also been conducted for turbulent flows, with $R_c = 10^6$, closed by the standard $k-\varepsilon$ two-equation model. For flows in the casing shown in Figs. 6 and 8, the solutions are shown in Fig. 10. For high Reynolds number flow, there is less influence of the mean pressure gradient along the circumferential direc-

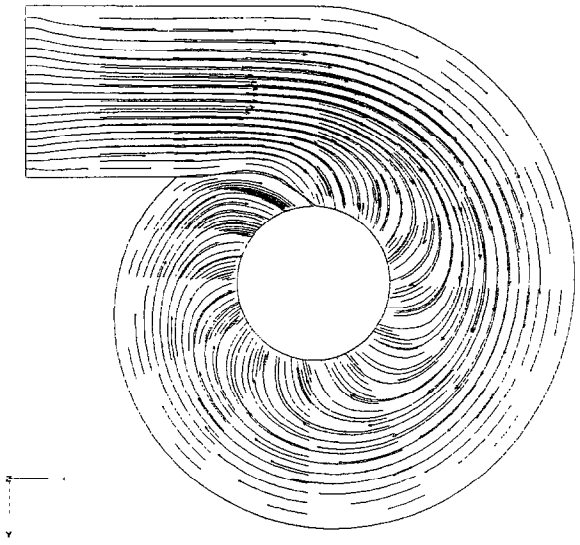

particle trajectories

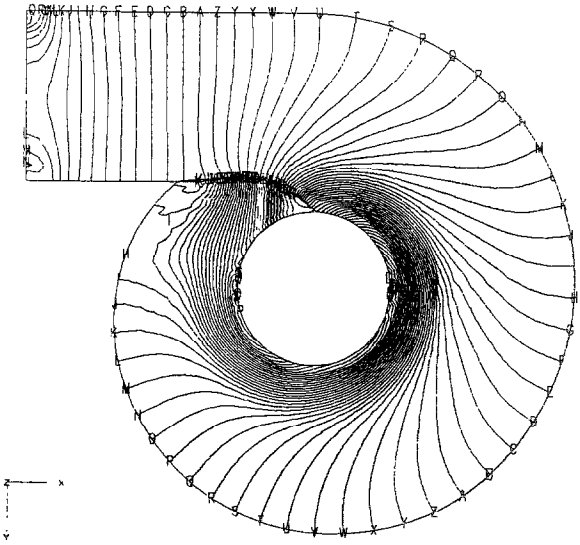

static pressure contours

FIG. 7. Solution of laminar flow (Re = 100) in a casing with smoothly varying wall contours.

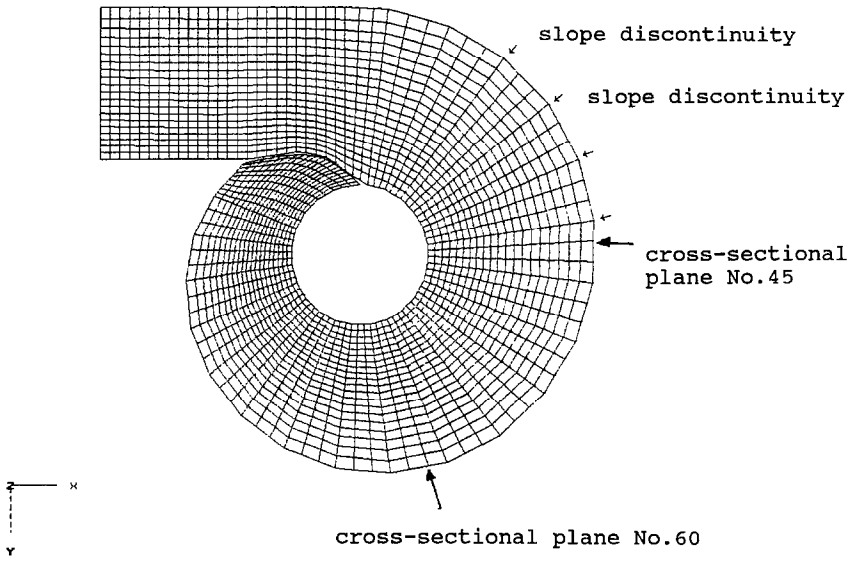

FIG. 8. Grid system in top-view plane of a casing with wall contours with 20 segmented straight lines encompassing 360°.

islands in the outer domain. These islands are *not* present in the flow through the smoothly turning geometry of Fig. 6. One implication here is that a conventional averaging procedure may eliminate these pressure oscillations caused by the aburpt turning of the casing wall which are inherent to the given design.

Figure 11 illustrates the evolution of the secondary velocity field of the turbulent flow on two selective cross sections, i.e., planes No. 45 and No. 60 (as indicated in Fig. 8). The combinations of centripetal force, no-slip condition along the solid walls, and the exit opening in the inner circumference cause the secondary flow to exhibit strong velocity in the top and bottom wall regions along with double swirls in the core region. The swirls in the core region are not only of much weaker strengths but also of gradually reduced sized toward downstream.

B. *Draft Tube*

The draft tube is a curved diffuser located beneath the turbine that delivers the exhaust flow from the turbine to the tailwater basin. The role of the draft tube is to reduce the velocity of the water existing from the turbine, thereby converting the excess kinetic energy of the exhaust water into a rise in static pressure. As shown in Fig. 12, a typical draft tube is characterized by a 90° turning as well as substantial increase of cross-sectional area from the inlet to the outlet. This flow configuration has been studied by the present algorithm as reported in [6, 15]. It should be pointed out that in [6], some cellular structures of the static pressure contours

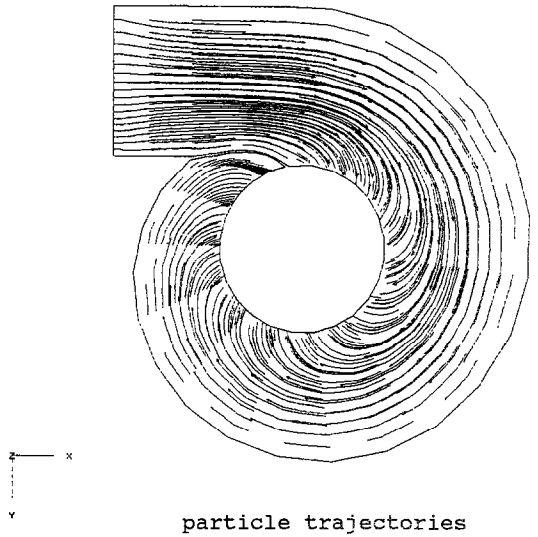

FIG. 9. Solution of laminar flow (Re = 100) in a casing with segmented straight-line contours. Note the effect of wall slope discontinuities on pressure distribution.

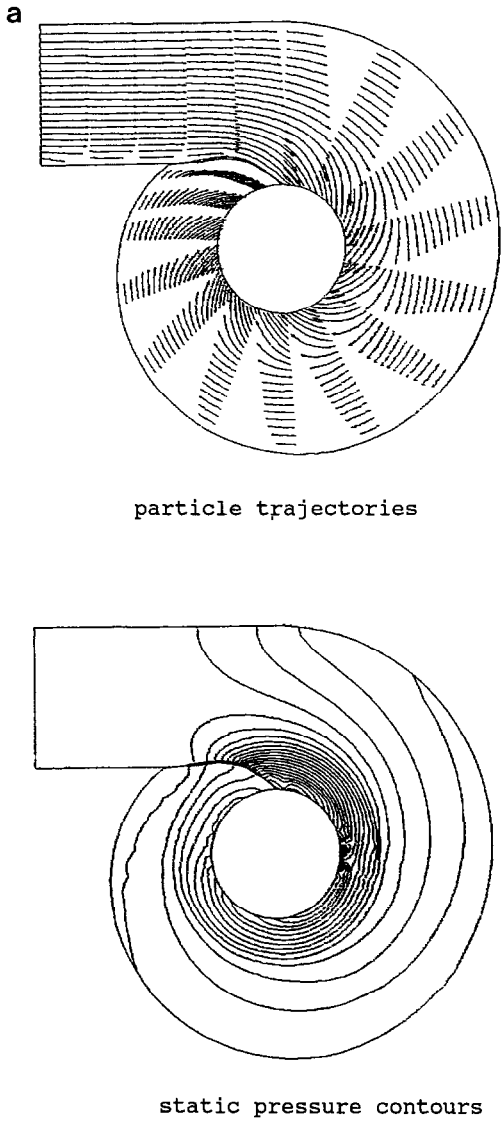

FIG. 10a. Solution of turbulent flow ($Re = 10^6$) in a casing with smoothly varying wall contours.

were observed downstream of the turning section. The reason for deserving these structures was not clear at the time of publication. Later on, it was found that these cellular structures were mainly caused by, again, the numerical definition of the flow configuration. In [6], the draft tube was first geometrically defined by some limited number of points along the through flow direction, and the geometry between any two points was defined by straight line interpolation. This practice was

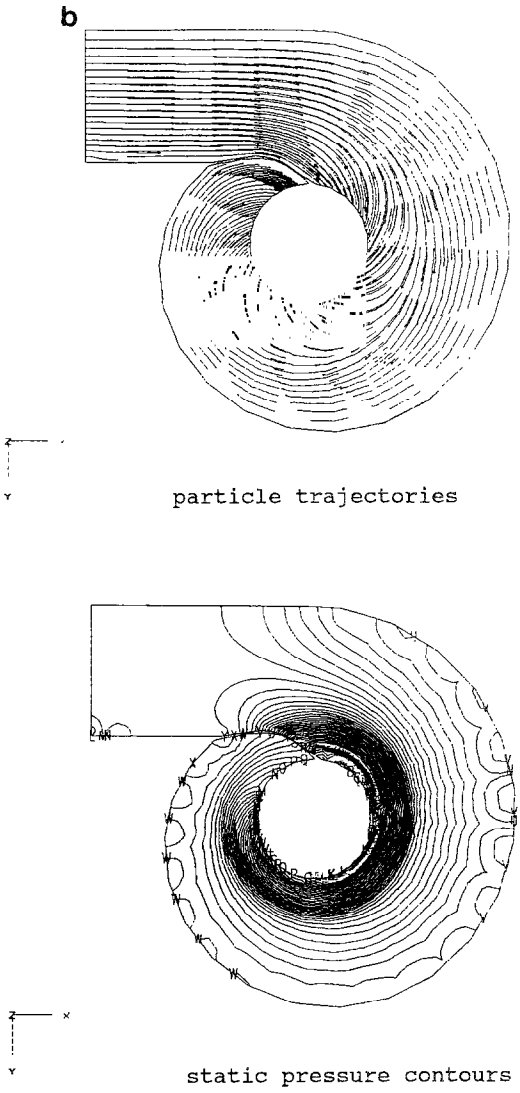

FIG. 10b. Solution of turbulent flow ($Re = 10^6$) in a casing with segmented straight-line contours. Note the effect of wall slope discontinuities on pressure distribution.

superseded later by a cubic spline interpolation and those cellular structures essentially disappear as a result of this improved geometry definition, as shown in Fig. 12 for a typical result of the flowfield computed in a grid system of $61 \times 19 \times 15$ nodes. Hence the apparent oscillations of the pressure field reported in [6] are caused not by the numerical algorithm but rather by the nonsmoothness of the discretized geometry used for computations.

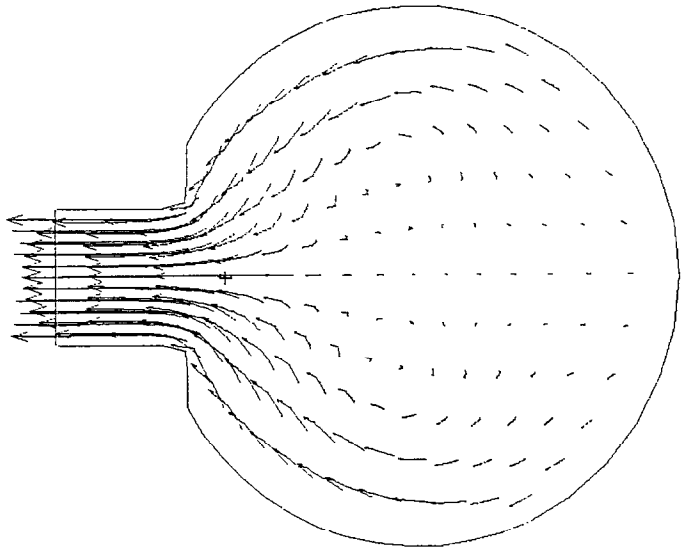

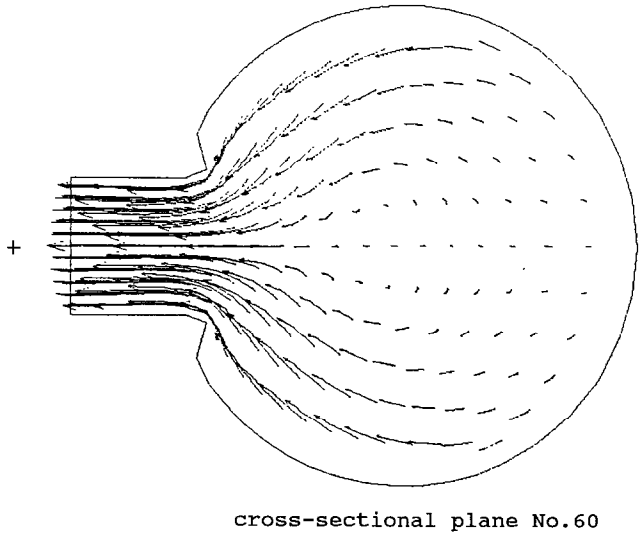

FIG. 11. Velocity pattern in two cross-sectional planes of turbulent flow ($Re = 10^6$) in a casing with segmented straight-line contours.

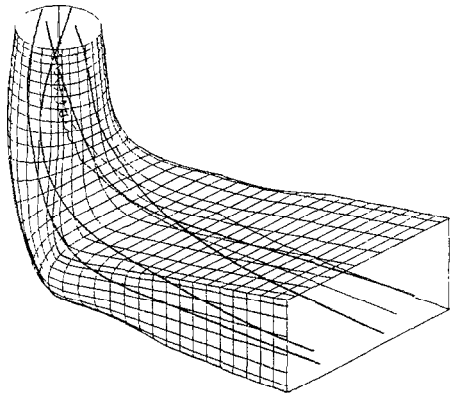

geometry and selected particle trajectories

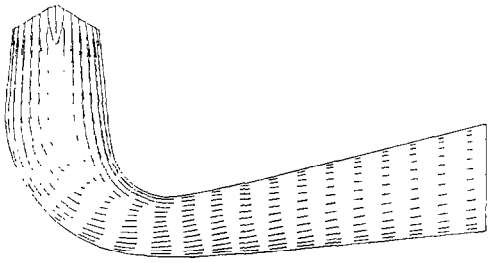

velocity vectors in middle side-view plane

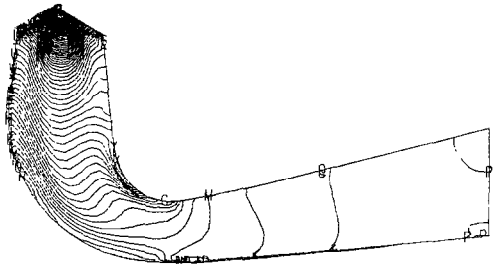

static pressure contours in middle side-view plane

FIG. 12. Geometry and solution of turbulent flow ($Re = 10^6$) in a draft tube with 90° turning.

4. SUMMARY AND CONCLUSION

The present work aims at investigating the issues of adopting the velocity variables and grid systems for computing the complex fluid flow in irregular geometries where the employment of a non-orthogonal curvilinear coordinate system is necessary. The following are some conclusions reached by the study.

(i) The strong conservation law in differential forms can be completely retained by the use of Cartesian velocity components. The use of the covariant or contravariant velocity components generally introduces source terms into the differential governing equations due to the curvature effects.

(ii) In the framework of the finite-volume approach, the momentum equations based on the Cartesian velocity components can satisfy the geometric conservation law in both convection and pressure terms. The second derivative (viscous) terms involve nonlinear metric terms and hence do not guarantee the satisfaction of the geometric conservation law. For the equations based on the curvilinear velocity components, the nonlinear metric terms appear both in the first and second derivative terms. Coupled with the curvature source terms, the utilization of the curvilinear velocity components as the primary variables makes the degree of satisfaction in terms of honoring the geometric conservation law more influenced by the grid skewness.

(iii) A unique issue facing the use of the Cartesian velocity components is that of 90° turning. It is demonstrated here that by combining with the staggered grid arrangement, the Cartesian velocity components can still perform satisfactorily even with the exact 90° turning. This can be achieved by defining the curvilinear coordinates (and hence the orientation of the flow domain) to be non-parallel to the Cartesian coordinates, or by utilizing the meshes of nonuniform spacings. In practice, satisfactory results have been obtained with the use of the Cartesian velocity components and the staggered grid system without introducing extra smoothing procedures, in all mesh shapes, as demonstrated in the examples given here and in the previous publications cited in the references.

(iv) In the context of curvilinear coordinates and with proper orientation or grid arrangement, the staggered grid can eliminate the need of devising any artificial smoothing terms to suppress the spurious oscillations. It can also naturally satisfy the pressure equation without introducing artificial boundary conditions. Nevertheless, it should be pointed out that the extrapolation procedure may still be needed for the pressure terms in the momentum equations.

(v) As a related issue, it is pointed out that the conventional manner of averaging the static pressure field may not be a good practice since there are engineering designs which inherently produce oscillations due to variations of wall contours.

It should be clear that as a result of the above discussions, there is no choice or algorithm that is perfect in all aspects. The present paper does not attempt to promote this. What has been attempted here is to clarify some of the confusing points found in the literature by both logical discussion and pragmatic demonstration and to point out the potential strength and weakness of each of the methods under consideration.

ACKNOWLEDGMENTS

The authors acknowledge the helpful comments made by the reviewers. Sincere thanks are due to Ms. Aileen Zimmerman for her expert typing. This research has been supported in part by Dominion Engineering Works.

REFERENCES

1. K. C. KARKI, Ph. D. thesis, University of Minnesota, 1986 (unpublished).
2. S. V. PATANKAR, *ASME J. Heat Transf.* **110**, 1037 (1988).
3. H. Q. YANG, K. T. YANG AND J. R. LLOYD, *Int. J. Numer. Methods Engng.* **25**, 331 (1988).
4. W. SHYY, S. S. TONG, AND S. M. CORREA, *Numer. Heat Transf.* **8**, 99 (1985).
5. M. E. BRAATEN AND W. SHYY, *Numer. Heat Transf.* **9**, 557 (1986).
6. W. SHYY AND M. E. BRAATEN, *Int. J. Numer. Methods Fluids*, **6**, 861 (1986).
7. S. V. PATANKAR, *Numerical Heat Transfer and Fluid Flow*, (Hemisphere, Washington, DC, 1980).
8. S. WITTIG, H. J. BAUER AND B. NOLL, in AGARD CP. No. 422, paper No. 28, 1988 (unpublished).
9. W. SHYY, *Comput. Methods Appl. Mech. Engng.* **53**, 47 (1985).
10. T. C. VU AND W. SHYY, *ASME J. Fluids Engng.* **110**, 29 (1988).
11. W. SHYY, S. M. CORREA, AND M. E. BRAATEN, *Combust. Sci. Tech.* **58**, 97 (1988).
12. W. SHYY AND P. Y. CHANG, *Int. J. Heat Mass Transf.* **33**, 495 (1990).
13. W. SHYY AND M. E. BRAATEN, "Proceedings First Nat'l Fluid Dynamics Congress," AIAA-3568-CP 1988 (unpublished)
14. W. SHYY, *Num. Heat Transf.* **14**, 323 (1988).
15. T. C. VU AND W. SHYY, *ASME J. Fluids Engng.* **112**, 199 (1990).
16. P. CONCUS AND G. GOLUB, *SIAM J. Num. Anal.* **10**, 1103 (1973).
17. R. L. SANI, P. M. GRESHO, R. L. LEE AND D. F. GRIFFITHS, *Int. J. Numer. Methods Fluids* **1**, 17, 171 (1981).
18. Y. S. CHEN, AIAA Paper No. 88–0417, 1988 (unpublished).
19. C. M. RHIE AND W. L. CHOW, *AIAA J.* **21**, 1525 (1983).
20. M. REGGIO AND R. CAMARERO, *Num. Heat Transf.* **10**, 131 (1986).
21. W. SHYY, *J. Comput. Phys.* **57**, 415 (1985).
22. R. PEYRET AND T. D. TAYLOR, *Computational Methods for Fluid Flow* (Springer-Verlag, New York, 1983).
23. C. K. CHU, in *Advances in Applied Mechanics*, Vol. 18, edited by C–S. Yih (Academic Press, New York, 1978).
24. R. B. BIRD, W. E. STEWART, AND E. N. LIGHTFOOT, *Transport Phenomena* (Wiley, New York, 1960).
25. K. K. KUO, *Principles of Combustion* (Wiley, New York, 1986).
26. D. E. ROSNER, *Transport Processes in Chemically Reacting Flow Systems* (Butterworths, Boston, 1986).
27. P. D. THOMAS AND C. K. LOMBARD, *AIAA J.* **17**, 1030 (1979).